Macromolecules

ARTICLE

pubs.acs.org/Macromolecules

Synthesis, Nanostructures and Properties of Sulfonated Poly(phenylene oxide) Bearing Polyfluorostyrene Side Chains as Proton Conducting Membranes

Mark Ingratta, Elin Persson Jutemar, and Patric Jannasch*

Department of Chemistry, Polymer & Materials Chemistry, Lund University, POB 124, SE-22100, Lund Sweden

Supporting Information

ABSTRACT: Graft copolymers with ionic backbones and hydrophobic fluorinated side chains have been prepared by using lithiated poly(2,6-dimethyl-1,4-phenylene oxide) (PPO) as a macroinitiator for anionic polymerization of 4-fluorostyrene. After grafting of the poly(4-fluorostyrene) (PFS) side chains, the PPO backbone was selectively sulfonated using trimethylsilylchlorosulfonate under mild and controlled conditions. Microscopy of solvent cast membranes revealed copolymer self-assembly into remarkably regular and well-ordered morphologies which, depending on the molecular structure, included lamellar and cylindrical arrangements of the proton conducting ionic nanophases. Thermal analysis indicated separate glass transitions of the PFS and PPO phases, and high thermal degradation temperatures of the membranes at approximately 220 and 300 °C for the H^+ and the Na^+ forms, respectively. The proton conductivity of fully hydrated acidic membranes was similar to that of Nafion, reaching above 0.2 S cm^{-1} at 120 °C. Compared at the same ion exchange capacity, the proton conductivity of the graft copolymer membranes was two times higher than that of a membrane based on an ungrafted sulfonated PPO. The study showed that it is possible to tailor and prepare proton-exchange membranes with well-ordered morphologies and high proton conductivity by employing graft copolymers with a sulfonated backbone bearing hydrophobic side chains.

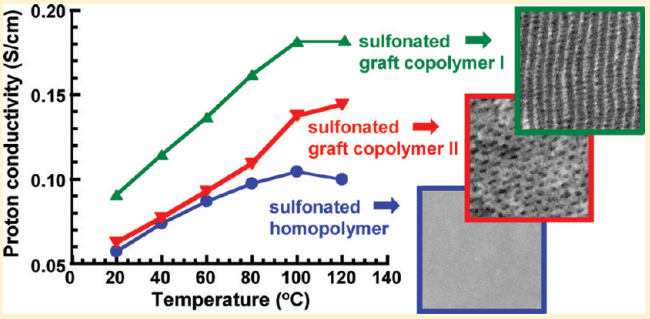

INTRODUCTION

The development of new alternative energy conversion technologies becomes increasingly important for many applications which today are dependent on fossil fuels. For example, fuel cell technology offers an attractive combination of high energy conversion efficiency and a potential for large reductions in power source emissions, including CO_2.[1,2] Proton-exchange membrane fuel cells (PEMFCs) are currently developed and adapted for a wide range of different applications and perhaps especially its introduction to the automotive sector promises to have a positive effect on the local and global environment. The core of the PEMFC is the membrane electrode assembly where oxygen and hydrogen react electrochemically on the two electrodes separated by the proton conducting membrane to directly and efficiently convert the chemical energy to electrical energy. The main challenges in the development and commercialization of PEMFCs are currently associated with performance, cost and lifetime—issues that are directly or indirectly related to the characteristics of the membrane.[3,4] Perfluorosulfonic acid (PFSA) membranes such as Nafion are still the benchmark and offer a good combination of performance and durability. Yet, the use of PFSA membranes brings limitations to PEMFC development because of their high cost and poor performance above approximately 80 °C and at relative humidities below approximately 40%.

During the past decade, a significant research effort has been aimed at developing new alternative membrane materials with improved properties and decreased cost.[5−11] These materials have for the most part been based on various durable hydrocarbon polymers; mainly on aromatic polymers with the ionic sulfonic acid groups distributed along the backbone (see Scheme 1b).[5] Generally, these polymers show poor ionic phase separation and cluster formation and only reach high proton conductivities at high ionic contents, leading to high water uptake and loss of dimensional stability. The membrane properties can be significantly improved by placing the ionic groups on short side chains (Scheme 1c).[12−15] This will generally result in a morphology with larger ionic phase domains (clusters) dispersed in a hydrophobic phase domain, which facilitates proton conductivity and stabilizes the membrane toward excessive swelling.[16]

Even larger ionic phase domains are obtained in ionic block and graft copolymers, where hydrophilic and highly ionic segments are combined with hydrophobic nonsulfonated segments.[9] These polymers have proved successful when it comes to promoting proton conductivity under low relative humidity while inhibiting excessive water swelling under immersed conditions. For example, several

Received: December 17, 2010
Revised: February 16, 2011
Published: March 14, 2011

Scheme 1. Graphical Representations of Various Sulfonated Copolymer Structures, Including (a) Perfluorinated Nafion, (b) a Typical Hydrocarbon-Based Ionomer with Sulfonic Acid Units along the Backbone, (c) Hydrocarbon-Based Ionomer with Short Sulfonated Side Chains, (d) a Fluorocarbon Backbone with Long Sulfonated Side Chains, and (e and f) the Copolymers of the Present Work Consisting of a Sulfonated Hydrocarbon Backbones with Fluorocarbon Side Chains[a]

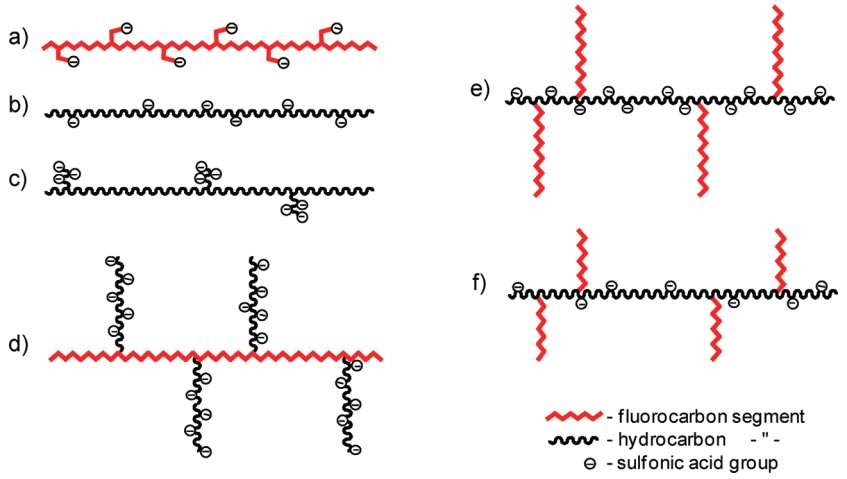

[a] Representations e and f help to illustrate the decreasing density of sulfonic acid groups along the backbone to maintain a constant ion exchange capacity as the side chain content is decreased.

types of hydrophilic−hydrophobic multiblock copolymers with regular nanostructured morphologies have been shown to have superior properties when compared to corresponding nonsegmented random copolymers.[17] However, the regular phase structure typically displayed by block copolymers can be a hindrance for proton conductivity. Recently, Holdcroft et al. compared the properties of diblock copolymers with those of graft copolymers having similar compositions and ionic contents.[18] The graft copolymer membranes were found to form an interconnected network of small ionic clusters similar to Nafion, which led to a controlled water uptake at high ionic contents. In contrast, the diblock copolymer membranes possessed a well-separated lamellar-like morphology which led to excessive water uptake at low ionic contents, as well as to anisotropic proton conductivity. Holdcroft and his group,[18−22] as well as others,[23] have synthesized and made detailed studies of several different graft copolymers where sulfonated polymeric side chains are attached to hydrophobic hydrocarbon or fluorocarbon backbones (Scheme 1d) with the aim to establish relationships between polymer microstructure, water uptake and proton conductivity.

In the present study we have prepared and investigated graft copolymers with hydrophilic sulfonated aromatic backbones and hydrophobic fluorocarbon side chains (Scheme 1e), i.e., the reversed placement of the ionic groups as compared with the graft copolymer studied by Holdcroft et al. This may have some advantages because each chain end of the ionic chain segment in-between the graft sites is attached to a hydrophobic side chain, which may impede the water uptake in relation to a graft copolymer with free ionic side chain ends. The molecular structures of the present graft copolymers provide the possibility to form various membrane morphologies depending on the phase ratio and the degree of sulfonation of the backbone. The synthetic strategy involved anionic polymerization of 4-fluorostyrene (FS) from a poly(2,6-dimethyl-1,4-phenylene oxide) (PPO) backbone, followed by mild and selective sulfonation of the PPO. This gave rise to ionic graft copolymers with a rather stiff sulfonated backbone which carried comparatively flexible hydrophobic side chains. The overall goal of the study was to investigate relationships between polymer structure, morphology, water uptake, and proton conductivity and to clarify if this particular polymer structure had an advantage over the ungrafted sulfonated PPO homopolymer in terms of proton conductivity.

EXPERIMENTAL SECTION

Materials. PPO in powder form was purchased from Sigma-Aldrich and was determined to have a number-average molecular weight (M_n) of 16.6 kg mol^{-1} and polydispersity ($M_w \times M_n^{-1}$) of 2.4 by size exclusion chromatography (SEC), using polystyrene standards in chloroform (see Structural Characterization). The polymer was dried in a vacuum oven for 24 h at 80 °C prior to use. Tetrahydrofuran (THF, Fischer Scientific, HPLC grade) was dried over molecular sieves (Acros; 4 Å, 8−12 mesh), which were activated at 250 °C for 24 h and cooled to room temperature in a vacuum oven prior to use. Nafion 117 (Alfa Aesar), methanol (Fischer Scientific; HPLC grade), *N*-methylpyrrolidinone (NMP; Acros; 99%), 1,1-diphenylethylene (DPE, Sigma-Aldrich, 97%), 4-fluorostyrene (FS, Sigma-Aldrich, 99%), trimethylsilylchlorosulfonate (TMSCS, Sigma-Aldrich, 99%) and trimethylchlorosilane (TMCS; Aldrich; 99+%) were all used as received. *n*-Butyllithium (*n*-BuLi, Acros; 2.5 M in hexanes) was used as received after titration to determine the exact concentration.[24]

Preparation of Poly(4-fluorostyrene) (PFS). PFS was prepared in order to study the sulfonation of this polymer under different conditions. A volume of 100 mL dry THF was added to a 250 mL round-bottom flask, which was then cooled to −70 °C, and degassed by vacuum/argon cycles seven times. Next, 0.6 mL (1.5 mmol) of 2.5 M *n*-BuLi was added, followed by 0.3 mL (1.70 mmol) of DPE. The solution immediately turned into a red-pink color. After 40 min, 2.5 mL (20.9 mmol) of degassed FS was added dropwise. The temperature increased slightly and the solution changed to a dark purple color. After 30 min, the reaction was quenched with methanol. The volume of THF was reduced using a rotary evaporator and the polymer was precipitated in 100 mL of methanol. The product was dried and precipitated from methanol a second time before analysis. The polymer was recovered as a white fluffy powder in 15% yield after the purification procedure. SEC analysis in chloroform showed a M_n of 20 kg mol^{-1} relative to polystyrene standards and the ^{1}H and ^{19}F NMR spectra confirmed the structure of the product (see Supporting Information, Figures SI.1, -3, and -4).

dx.doi.org/10.1021/ma102879w |*Macromolecules* 2011, 44, 2074–2083

Scheme 2. Synthetic Pathway for Grafting PFS Side Chains from a PPO Backbone by Anionic Polymerization Followed by Controlled and Selective Sulfonation Using Trimethylsilylchlorosulfonate

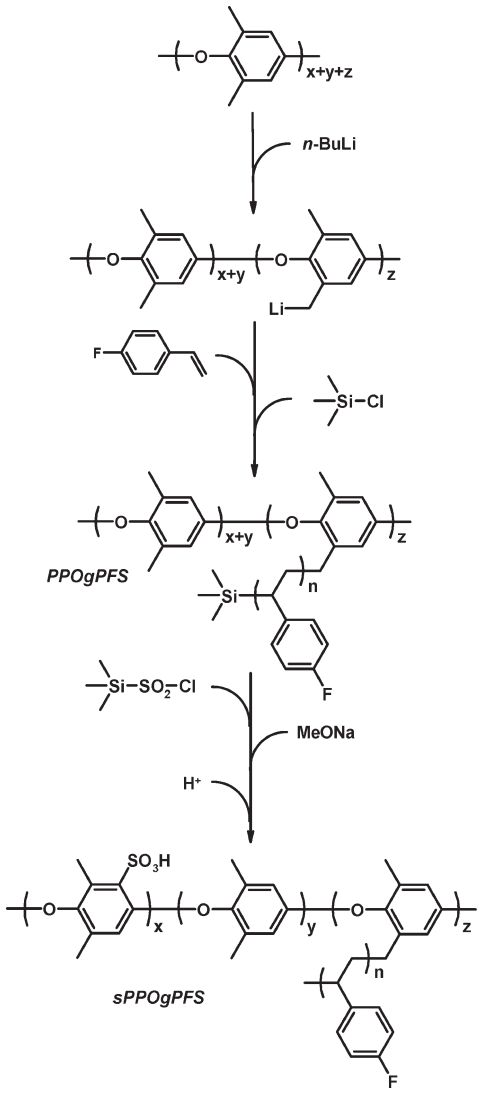

Preparation of Poly(phenylene oxide)-*graft*-poly(4-fluorostyrene) (PPOgPFS). Three copolymers were prepared according to Scheme 2 with a similar number of grafting sites, but with different lengths of the PFS side chains. First, a 4-neck 250 mL round bottomed flask with thermometer, septum, argon inlet and stir bar was charged with 0.500 g (corresponding to 4.17 mmol repeat units) of PPO and 150 mL of dry THF. The heterogeneous mixture was cooled to −30 °C, placed under vacuum followed by argon addition seven times. The solution was then heated to 60 °C to fully dissolve the PPO before cooling once more to 22 °C. Next, *n*-BuLi solution was added dropwise. A small volume was first used to consume traces of impurities present, after which the solution became bright yellow-orange in color. Then, 0.3 mL (0.750 mmol) of *n*-BuLi was added to lithiate the PPO, which corresponded to 15% of the repeat units. After 10 min at room temperature, the solution was cooled to −70 °C for 20 min. Degassed FS was then added all at once, and the solution immediately changed to a deep orange-red color. Amounts of 0.410 g (3.35 mmol), 0.676 g (5.45 mmol), and 1.02 g (8.38 mmol) of FS were charged to prepare copolymer samples PPOgPFS1, -2, and -3, respectively. After 20 min, the polymerization reaction was terminated by adding 1 mL (7.88 mmol) TMCS. The solution was left to warm to room temperature before the product was first concentrated using a rotary evaporator and then precipitated in methanol to form a white fluffy powder. The yield was quantitative and thus essentially all of the charged FS was incorporated in the copolymers. ^{1}H and ^{19}F NMR spectroscopy data was used to calculate the amounts of PFS present, and the results agreed well with the monomer feed. The number of grafted chains was estimated from the trimethylsilyl peaks.[30−32]

Sulfonation of PFS, PPO, and PPOgPFS. A typical sulfonation reaction was completed as follows. A one neck 50 mL round-bottom flask with stir bar was charged with 25 mL of dry chloroform and 250 mg of polymer. The desired amount of TMSCS was added dropwise at room temperature. The solution immediately turned clear yellow, with a precipitate forming after several hours depending on the PPO:PFS ratio of the polymer. The higher the PFS content, the longer the polymer remained soluble. After 24 h, sodium methoxide and methanol were added and the solution was stirred for 3 h. Chloroform was removed using a rotary evaporator and 50 mL of water was added and the solution was stirred 18 h. The white swollen precipitate was filtered and dried at 80 °C in a vacuum oven. Next, chloroform was added and the solution was stirred for 5 h to remove any homo-PFS fraction remaining from the preparation of PPOgPFS. The swollen precipitate was then filtered out and the sulfonated samples were finally dried at 80 °C under vacuum.

Membrane Preparation and Characterization. An amount of 0.15 g of sulfonated polymer was dissolved in 3 g of NMP during gentle heating. The solution was filtered into a Petri dish which was placed into an oven at 90 °C under a blanket of N_2 for 24 h. The membrane was then transferred into an oven at 80 °C under vacuum to remove residual solvent. After swelling it in water to make it detach from the Petri dish, the membrane was acidified by immersion into 50 mL of 1 M HCl at room temperature during 24 h. Next, residual HCl was removed through several washes with deionized water over 24 h. The membrane was then placed into 50 mL of 1 M NaCl for 48 h. The membrane was removed and washed with deionized water which was combined with the NaCl solution. The NaCl solution was titrated with a 0.001 M NaOH solution to determine the amount of accessible acid groups within the membrane. The membrane was finally dried at 80 °C under vacuum to determine the dry weight which was used to calculate the ion exchange capacity (IEC) in mmol H^+ per gram of dry polymer membrane.

The water uptake (w_{water}) was determined according to eq 1 for the sulfonated polymer membranes after casting. Dry weights (W_{dry}) were determined after drying the membranes in a vacuum oven at 80 °C for 24 h while wet weights (W_{wet}) were determined by immersing the membrane in Milli-Q water for 24 h. The wet membranes were weighted after excess water was removed quickly using tissue paper.

$$w_{water} = [(W_{wet} - W_{dry}) \times W_{dry}^{-1}] \times 100\% \quad (1)$$

Structural Characterization. ^{1}H NMR and ^{19}F NMR analysis was completed using a Bruker 400 MHz spectrometer. Spectra of the PPOgPFS copolymers and their sulfonated derivatives were recorded using $CDCl_3$ and DMSO-d_6 solutions, respectively. The content of PFS was calculated for the unsulfonated copolymers by comparing the integral of the benzyl protons of PPO at 2.1 ppm ($I_{2.1}$) relative to the integrated signal of the protons in the aromatic region that arose from PFS and the PPO backbone ($I_{6.3-6.9}$) according to eq 2:

$$\text{mol\%PFS} = \frac{I_{6.3-6.9} - [2 \times (I_{2.1}/6)]}{4} \quad (2)$$

The peaks from the methyl groups of TMS were used to quantify the number and distribution of active lithiated sites at the end of the grafting reaction, and appeared at 0.45 ppm for Ar−Si$(CH_3)_3$, and −0.069 ppm for PFS−Si$(CH_3)_3$ and ArCH_2−Si$(CH_3)_3$. The degree of

substitution (DS) was calculated as shown in eq 3:

$$DS = \frac{I_{-0.7}/9}{I_{2.1}/6} \quad (3)$$

It was not possible to determine the composition of the sulfonated PPOgPFS copolymers by ^{1}H NMR spectroscopy due to the complex overlap of the shifts related to sulfonated and unsulfonated PPO units, and PFS. Instead, the PFS content of the copolymers was estimated by ^{19}F NMR analysis of PPOgPFS before and after sulfonation and purification. Hexafluorobenzene (HFB) was used as an internal standard because it had a strong signal in the aromatic region close but not overlapping that of PFS. The HFB and PFS fluorines were both singlets, located at −164.9 and −119.7 ppm relative to $CFCl_3$, respectively. To determine whether the spectral signal was comparable between the fluorines attached to the copolymer and the small molecule HFB, several solutions containing known amount of PFS homopolymer and HFB were examined to determine the experimental ratio of the fluorine peaks compared to the expected values of the number of moles added. It was found that the spectral signal from the fluorine of the PFS was 13 ± 3% and 47 ± 4% different in DMSO-d_6 and $CDCl_3$, respectively, than expected from the molar ratios of the known amounts added. Thus, when comparisons were made between the fluorine signals from the PPOgPFS copolymer and HFB, the signal from the PFS fluorine was adjusted to compensate for the difference in spectral yield. In a typical experiment, a known amount ranging from 5 to 10 mg of copolymer and a known amount of approximately 5−10 mg of HFB were added to 1.0 mL of DMSO-d_6 or $CDCl_3$.

FTIR analysis was completed using a Bruker IFS 66 spectrometer. The dry polymer samples were ground together with KBr and pressed into tablets. The spectra were recorded from 400 to 4000 cm^{-1} with a resolution of 2 cm^{-1} after 128 scans.

SEC analysis of the unsulfonated PPO and graft copolymers was performed using Waters SEC equipped with Shodex KF−805, KF−804 and KF−802.5 columns in series, a Viscotek refractometer, model 250, and with chloroform as the mobile phase at a flow rate of 1 mL min^{-1}. The sulfonated polymers were not soluble in chloroform and thus analysis was performed using a Waters 2695 Separations Module equipped with a Waters 2414 Refractive Index Detector and two PLgel 5 μm mixed-D (300 mm ×7.5 mm) columns connected in series. Samples were dissolved in DMF with 10 mM LiBr and 1% (v/v) NEt_3 at 85 °C and were injected at a flow rate of 1 mL/min and calibrated against polystyrene standards. Using DMF containing a lithium salt has been shown to aid in the SEC analysis of polyelectrolytes.[33]

Transmission Electron Microscopy. TEM samples were prepared using the following steps: Membranes (∼100 nm) were ion-exchanged to Pb^{2+} by immersion in a 1 wt % solution of lead acetate. The films were rinsed with water and dried in vacuum at 80 °C for 48 h. The dry membranes were embedded in Spurr's epoxy resin and the blocks were sectioned to yield slices with a thickness of 30−50 nm using a microtome. After picking up the slices on glow discharge treated lacey carbon grids, images were taken on a Philips CM120 BioTWIN CRYO transmission electron microscope using an accelerating voltage of 120 kV.

Thermal Analysis. Thermogravimetric analysis (TGA) was conducted using a Q500 thermogravimetric analyzer from TA Instruments. Polymer thermal stability was measured under N_2 for membranes in both the sodium and protonated form, as well as under air for membranes in the protonated form up to 600 °C. A scan rate of 10 °C min^{-1} and 1 °C min^{-1} was used for measurements under N_2 and air, respectively. The polymers were predried at 150 °C for 10 min prior to the scanning cycle. The temperature at which the polymer had lost 5% of its original weight during the heating was taken as the degradation temperature (T_d).

Differential scanning calorimetry (DSC) was used to determine the glass transition temperatures (T_gs) for all membranes and was performed using a TA Instruments Q1000 DSC. Each sample was examined using the following sequence of scans: 40−240−50−300−50 °C. The heating and cooling rates were 10 °C min^{-1} and the reported T_gs were determined from the last heating scan.

Proton Conductivity Measurements. The proton conductivity was evaluated by electrochemical impedance spectroscopy (EIS) using a Novocontrol V 1.01S high-resolution dielectric analyzer equipped with a Novocool temperature system. Samples were equilibrated under immersed conditions before being placed into the closed cell electrode for EIS measurements. In-plane conductivity was measured on an 8 × 8 mm membrane clamped between two stainless steel electrodes. Impedance data was collected between 10^{-1} and 10^7 Hz at a voltage amplitude of 50 mV from −20 to +120 °C. The conductivity was determined by plotting the imaginary part of the conductivity vs the real part, and the conductivity was taken as the real value corresponding to the minimum imaginary response.

RESULTS AND DISCUSSION

Tailoring of Graft Copolymers. In the present work, we have prepared graft copolymers with hydrophilic sulfonated aromatic backbones and hydrophobic fluorocarbon side chains according to Scheme 2. In this synthetic approach, a mild sulfonation procedure was applied on a graft copolymer having electron rich aromatic rings activated for sulfonation in the backbone, and electron poor aromatic rings deactivated for sulfonation in the side chains. PPO was chosen as the backbone because of the electron donating effects of the oxygen and methyl substituents on the aromatic ring, facilitating the introduction of sulfonic groups by electrophilic substitution. Moreover, there are many possibilities to graft PPO, e.g., by anionic or controlled radical polymerizations, by utilizing its aromatic or benzylic positions.[25] FS was chosen as the building block for the side chains because it polymerizes through an anionic mechanism,[26] and the aromatic ring of PFS contains an electron withdrawing fluorine substituent, thus deactivating it toward sulfonation.

Since mild sulfonation conditions were desired, the sulfonation of PPO was performed by using TMSCS in chloroform.[34−37] This method for sulfonation is advantageous not only due to the potential selectivity for sulfonation of the PPO, but also because the PPO will remain soluble for a longer time during the sulfonation reaction. The polymer will thus predominantly be homogenously sulfonated and will have more evenly distributed sulfonate groups compared polymers sulfonated using harsh methods including the use of refluxing sulfuric acid.[27]

In order to experimentally determine the conditions at which sulfonation occurs selectively on the PPO aromatic rings, and not on PFS, an initial study of the sulfonation of a PFS homopolymer was carried out. Two sulfonation reactions were completed with different molar ratios of PFS repeat unit to TMSCS. The first sulfonation with [PFS]:[TMSCS] = 1:1 to produce sample s1PFS was considered to be a realistic reaction condition to be used for the PPOgPFS copolymers, and the second with [PFS]:[TMSCS] = 1:5 to produce sample s2PFS was carried out to evaluate the resistance of PFS toward sulfonation. Both samples were examined using ^{1}H NMR spectroscopy, TGA, and DSC.

After purification, sample s1PFS showed no differences in thermal properties, in solubility, or in the ^{1}H NMR spectrum in relation to the starting material. On the other hand, the properties of sample s2PFS had changed markedly in relation to the starting material. For example, the thermal analysis showed a degradation weight loss beginning at approximately 273 °C, which was approximately 100 °C below that of the original PFS. In addition, a significant increase in the T_g was noted, from 108 °C for the starting material up to 175 °C for sample s2PFS.

Table 1. PPOgPFS Copolymer Data

copolymer	PFS content by ^{1}H NMR (wt %)	PFS content by ^{19}F NMR (wt %)	DS[a]	M_n of PFS side chain (g mol^{-1})	T_{g1} (°C)	ΔC_{p1} (J g^{-1} K^{-1})	T_{g2} (°C)	ΔC_{p2} (J g^{-1} K^{-1})	$T_{d,5\%}$[b] (°C)
PPOgPFS1	47	44	0.03	3400	109	0.113	208	0.120	404
PPOgPFS2	57	56	0.03	4900	112	0.140	214	0.098	409
PPOgPFS3	67	64	0.04	4400	113	0.163	204	0.081	405

[a] Fraction of PPO repeat units that were grafted with PFS side chains, as determined by NMR analysis of the TMS modified PFS side chain ends. [b] Measured under N_2 at 10 °C min.$^{-1}$ heating rate.

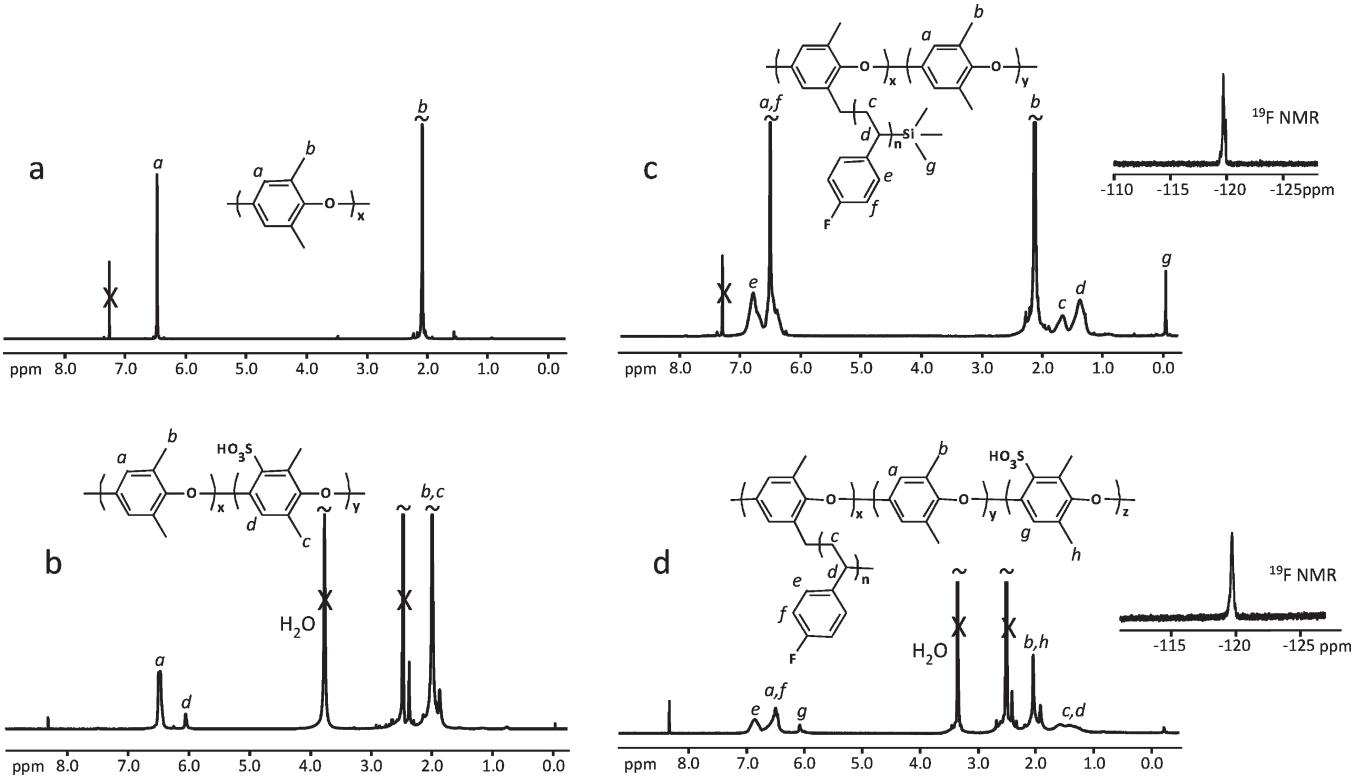

Figure 1. ^{1}H NMR spectra of PPO (a), sPPO (b), PPOgPFS1 (c), and s1PPOgPFS1 (d). The data of the sulfonated and nonsulfonated polymers were recorded using DMSO-d_6 and $CDCl_3$ solutions, respectively. The insets in part c and d show the corresponding ^{19}F NMR spectra.

The solubility also changed significantly; sample s2PFS was no longer soluble in chloroform, but remained soluble in dimethyl sulfoxide. These initial experiments showed that sulfonation of PFS would occur if sufficiently harsh conditions were employed. For this reason, the sulfonation reaction conditions of the copolymers were kept under mild conditions where no, or only very little, sulfonation of PFS was expected to occur.

Synthesis and Structural Characterization of PPOgPFS. Anionic polymerization was chosen for the grafting polymerization from PPO due to the ease of a one pot synthesis, compared to other recent studies involving the synthesis of graft copolymers via atom transfer radical polymerization.[28,29] As found previously, lithiation of the PPO backbone using *n*-BuLi results in an anionic site reactive enough to initiate polymerization of styrene[30,31] and vinylphosphonic acid.[32] Three PPOgPFS copolymers were prepared in the present work; all with a similar number of grafting sites and with different chain lengths of the PFS grafts (Table 1). The wt % PFS was calculated from both ^{1}H and ^{19}F NMR data and ranged from 47 to 67 wt %, with the ^{19}F NMR data giving slightly lower values than the ^{1}H NMR data. The ^{1}H NMR spectra of the starting PPO material and PPOgPFS1 are shown in Figure 1, parts a and c, respectively, with broad new peaks in the latter spectrum attributed to the aromatic protons of PFS at 6.4 and 6.8 ppm, as well as the aliphatic backbone protons at 1.3 and 1.7 ppm. By combining the molecular weight of the PPO obtained by SEC with the PFS content obtained by ^{1}H NMR spectroscopy, the molecular weights of the graft copolymers were calculated to be 31, 39, and 50 kg mol^{-1}, respectively. Direct SEC analysis of the copolymers showed increasing molecular weights in relation to the PPO backbone precursor, as well as very small amounts of PFS homopolymer formed (see Figure SI.1, Supporting Information), similar to what has been seen with PPO-*graft*-polystyrene.[30,31] Since the solubility of the nonsulfonated graft copolymer and that of the PFS homopolymer were very similar, PFS homopolymer was removed after the sulfonation when the two polymers had greatly different solubility characteristics.

The FTIR spectrum of PPOgPFS2 is shown in Figure 2b. As seen, several new peaks from the PFS component of the

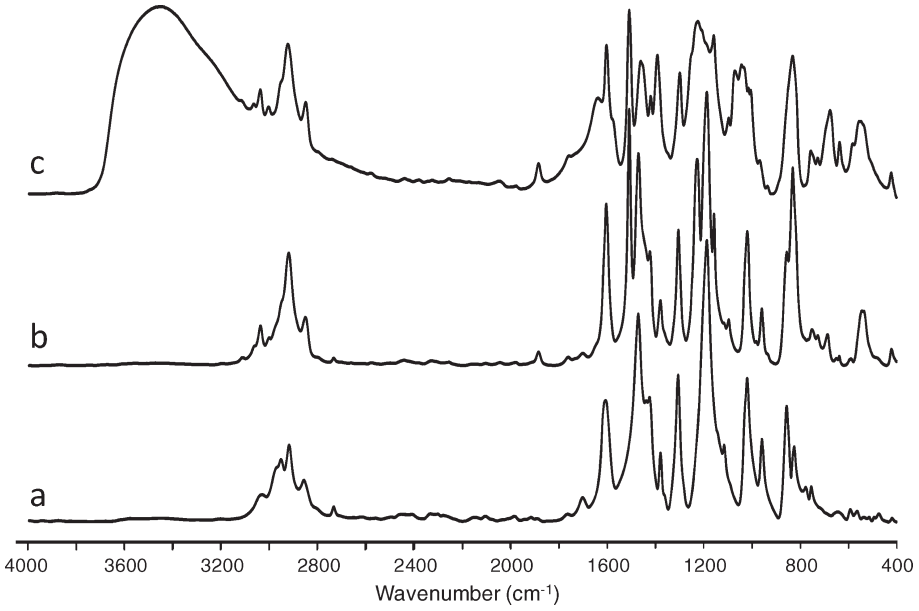

Figure 2. FTIR spectra of PPO (a), PPOgPFS2 (b), and sPPOgPFS2 (c).

Table 2. Data of Sulfonated Polymers and Membranes

sample	PFS content by ^{19}F NMR (wt %)	molar ratio [PPO]: [TMSCS]	IEC by titration (mmol g^{-1})	sulfonated PPO repeat units[a] (%)	water uptake[b] (wt %)	λ[c]	T_{g1} (°C)	$T_{d,5\%}(N_2)$[d] (°C)	$T_{d,5\%}$(air)[e] (°C)	σ(120 °C)[f] (S cm^{-1})
sPPO	-	1.0:0.4	1.2	16	20	9	-	298	302	0.10
s1PPOgPFS1	n.d.[g]	1.0:1.0	1.2	27	57	26	112	220	197	0.20
s2PPOgPFS1	n.d.[g]	1.0:2.0	1.4	36	70	28	112	256	208	0.25
sPPOgPFS2	56	1.0:1.0	1.2	41	50	23	114	265	248	0.18
sPPOgPFS3	67	1.0:1.0	1.0	45	32	18	114	246	230	0.14

[a] Calculated by using the percentage of PFS in the copolymers and the IEC value of the corresponding membrane. [b] Immersed in water at 20 °C. [c] $[H_2O]/[-SO_3H]$. [d] Measured at 10 °C min.$^{-1}$ heating rate. [e] Measured at 1 °C min.$^{-1}$ heating rate. [f] Measured under immersed conditions. [g] n.d.: not determined because of poor spectra.

copolymer are present at 829, 1224, and 1510 cm^{-1}, compared to the spectrum of PPO in Figure 2a. In addition, the aryl and saturated C−H bands between 3100 and 2800 cm^{-1} are changed after the grafting of PFS.

Sulfonation of PPOgPFS. Several copolymers were selectively sulfonated to investigate properties such as the level of organization of the ionic phase, thermal stability and conductivity of membrane polymers with sulfonated backbones and unsulfonated grafted side chains. The IEC values of the copolymers were kept close to 1.2 mmol g^{-1} polymer in order to have a common basis for comparison (Table 2). As shown in Scheme 1, parts e and f, maintaining a constant IEC while increasing the PFS content has the effect of increasing the percentage of sulfonated PPO repeat units in the backbone, as seen in Table 2. Sulfonation was confirmed by ^{1}H NMR and FTIR analysis, as shown in Figures 1d and 2c, respectively. A comparison of parts c and d of Figure 1 illustrated that the signal from the aromatic protons correlated to PPO decreased dramatically and that a new peak appeared at 6.1 ppm. The new peak at 6.1 ppm corresponded to the Ar−H at the meta position to an sulfonate group attached to PPO. This was confirmed by comparison with sulfonated PPO (sPPO) synthesized in the current work, as shown in Figure 1b. The degree of sulfonation was calculated for sPPO using the peak ratios for the sulfonated and nonsulfonated aromatic rings of PPO and was found to be 1.2 mmol g^{-1}. However, the IEC values for the PPOgPFS copolymers could not be determined in this fashion due to peak overlap in both the aromatic and aliphatic regions. Instead, the IEC was determined by titration for all the sulfonated samples. In the case of sPPO, the IEC determined by ^{1}H NMR and titration were identical, thus indicating that the majority of sulfonate groups were accessible to the acidified solution. The IEC values for all samples are shown in Table 2, and were all close to 1.2 mmol g^{-1} polymer.

Because of overlapping peaks, it was not possible to evaluate the PFS content of the sulfonated graft copolymers by ^{1}H NMR spectroscopy. Instead, efforts were made to evaluate the PFS content by ^{19}F NMR spectroscopy after the purification by leaching with chloroform and the subsequent membrane preparation. Possibly because of solubility reasons, it was not possible to determine the PFS content of the sulfonated copolymers derived from PPOgPFS1. Despite several analyses, the signal-to-noise ratio remained low for these copolymers and the results became very sensitive to the exact position of the integration limits. Still, comparing the data in Tables 1 and 2, the calculated wt % of PFS for the copolymers derived from PPOgPFS2 and PPOgPFS3 did not change significantly, indicating that only very little PFS homopolymer was formed during the grafting. A representative ^{19}F NMR spectrum of sPPOgPFS3

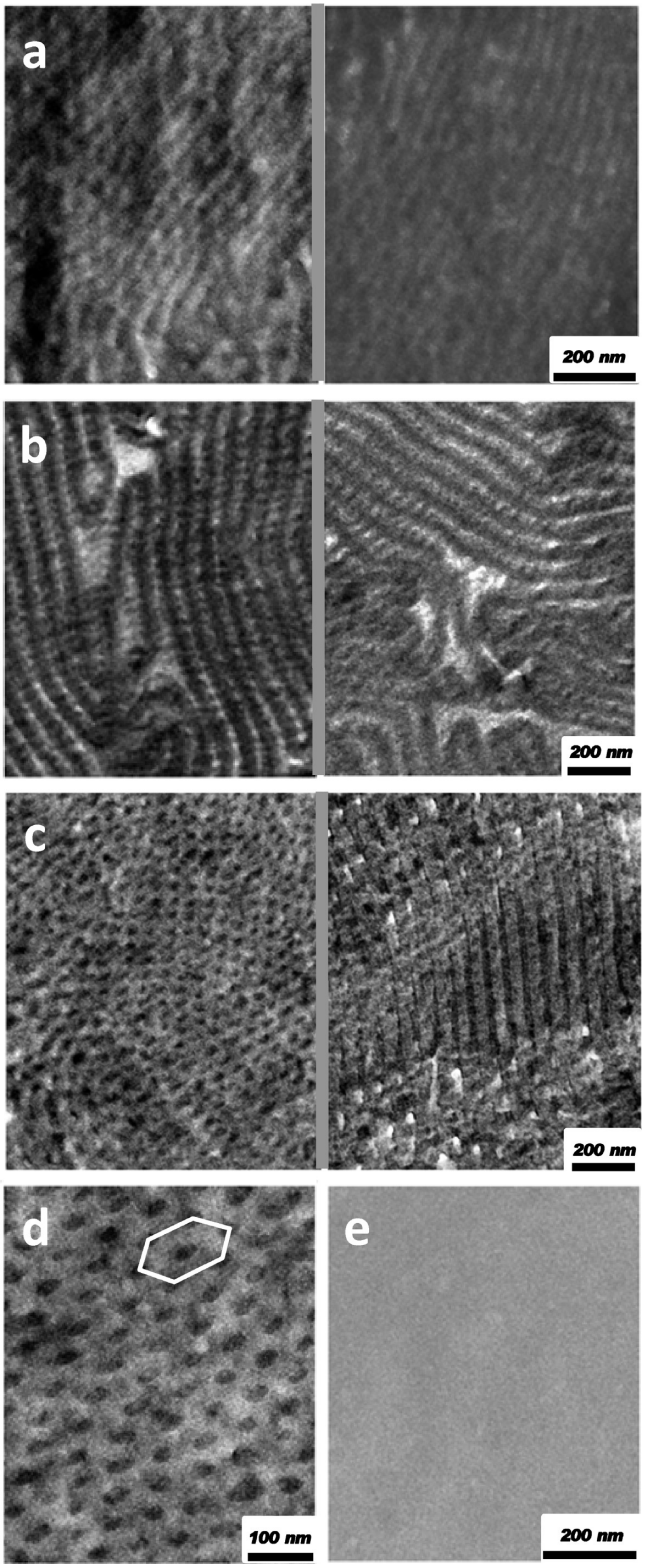

Figure 3. TEM images of s1PPOgPFS1 with 36 wt % PFS (a), sPPOgPFS2 with 56 wt % PFS (b), sPPOgPFS3 with 67 wt % PFS (c and d), and sPPO (e). The dark areas represent the ionic phase domains and the hydrophobic phase domains appear brighter. The white lines in image d indicate the hexagonal order of the cylinders.

spiked with HFB as an internal standard is shown in the Supporting Information (Figure SI.5). Furthermore, SEC analysis of the sulfonated copolymers with LiBr/DMF as the eluent showed a single peak in most cases, with only a very small amount of PFS homopolymer remaining for sPPOgFPS2 (see Figure SI.2, Supporting Information).

Figure 2c shows a representative FTIR spectrum of the sulfonated graft copolymers. New peaks attributed to the sulfonate groups are seen at 671, 1064, and 1390 cm^{-1}, confirming the presence of sulfonate groups attached to the copolymer. In addition, a broad O−H stretching band appeared between 3800 and 2800 cm^{-1}, most likely indicating the presence of water attracted by the hygroscopic sulfonate groups.

Membrane Morphology. Clear transparent membranes were cast from NMP solutions of the sulfonated polymers at 90 °C. Membranes s1PPOgPFS1, sPPOgPFS2, and sPPOgPFS3 had approximately the same DS and IEC, but different M_n of the PFS side chains and thus different PFS content (Table 2). Along with membrane sPPO, these membranes were selected for the TEM investigation to study the effect of copolymer structure on the ionic segregation and nanostructure of the membranes. In order to enhance the contrast between the phases, the membranes were ion-exchanged to their Pb^{2+} form before the TEM investigation. Thus, in the TEM images shown in Figure 3, the ionic phase domains appear as dark regions and the hydrophobic phase areas as brighter regions. As seen, all the copolymer membranes were distinctly phase separated and displayed various nanostructures, a consequence of the incompatibility between the ionic PPO backbone and the PFS side chains and the molecular structure of the respective copolymer.

Membrane s1PPOgPFS1 with the shortest PFS side chains of the investigated membranes revealed an arrangement of primarily lamellar phases with a periodicity of approximately 40 nm (Figure 3a). The membrane seemingly had a perforated lamellar morphology where the ionic phase partly penetrated the hydrophobic lamellae. Membrane sPPOgPFS2 contained 56 wt % PFS and the TEM images shown in Figure 3b displayed a distinct lamellar morphology. Although the lamellas showed recurrent curvature, they were regular with a periodicity of approximately 75−80 nm. Thus, the size of the phases was larger in sPPOgPFS2, as compared with s1PPOgPFS1, which was expected from the longer side chains of the former copolymer. The TEM images of membrane sPPOgPFS3, containing 67 wt % PFS, revealed a morphology with hexagonally close packed cylinders of the ionic phase in a matrix of the hydrophobic phase. The left image shown in Figure 3c shows cylinders oriented perpendicular to the plane of the sample surface, and the image to the right shows cylinders oriented in the plane of the sample surface. As seen in Figure 3d, the cylinders had a diameter of approximately 25 nm and their center-to-center distance was approximately 120 nm. As expected, membrane sPPO lacked the phase separated nanostructure of the copolymers and the TEM images were featureless (Figure 3d).

The morphologies displayed by the ionic graft copolymer membranes, as shown for example in Figure 3d, had remarkably regular phase sizes and ordered nanophases, almost comparable with those normally only displayed by linear block copolymers. The morphologies observed were for example very much different from those observed for poly(vinylidene difluoride-*co*-chlorotrifluoroethylene) grafted with partly sulfonated polystyrene side chains by Holdcroft et al.[18] These membranes displayed disordered phase separated morphologies with small and seemingly interconnected ionic clusters from 2 to 4 nm in size. In addition, the morphology of the present membranes were much more

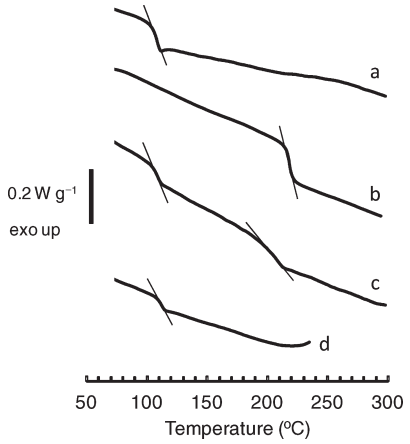

Figure 4. DSC heating scans of PFS (a), PPO (b), PPOgPFS1 (c), and s1PPOgPFS1 (d), recorded at 10 °C min^{-1}. The thin lines indicate the glass transitions.

regular and well-ordered than that displayed by sulfonated multiblock copolymers prepared by polycondensation and coupling reactions.[9] The higher degree of molecular organization in the present membranes was possibly due to the presumably low polydispersity of the anionically polymerized side chains which induced the phase regularity. The proton and water transport properties of the membranes may be further enhanced by employing techniques to align the ion-containing cylindrical and lamellar domains perpendicular to the plane of the membrane.[38]

Thermal Properties. Blends of the homopolymers PPO and PFS are known to be immiscible,[39] and thus display two glass transitions due to phase separation. Figure 4 shows the final DSC heating scans of PPO, PFS, PPOgPFS1 and s1PPOgPFS1, respectively. The T_g of the homopolymers PFS and PPO were determined to be 108 and 218 °C, respectively. The corresponding change in the specific heat (ΔC_p) in connection with the glass transitions were 0.246 and 0.240 J g^{-1} K^{-1}, respectively, for the two polymers. The unsulfonated graft copolymers all showed two distinct T_g values, T_{g1} at approximately 110 °C for the PFS phase and T_{g2} between 204 and 214 °C for the PPO phase (Table 1). Thus, the T_g values were close to those of the respective homopolymer which showed the very high degree of immiscibility of the PPO backbone segments and the PFS side chains. As expected, the values of ΔC_p increased with the respective content (Table 1). After sulfonation, T_{g1} for the PFS phase remained unchanged (Table 2), while no T_{g2} for the sulfonated PPO phase was detected below the degradation temperature of the copolymer above 240 °C. Sulfonated aromatic polymers are known to have increased T_g values compared to the corresponding unsulfonated polymers. The fact that the T_{g1} of the PFS phase remained unchanged strongly indicated that the sulfonation only occurred on the PPO backbone since sulfonation of PFS was shown to give an increase in the T_g.

The thermal stability of the membranes was examined by TGA for membranes in both the acid and sodium salt forms, under nitrogen and air. In Figure 5a, the TGA traces of PPO, sPPO, and the unsulfonated and sulfonated copolymers are compared in the sodium form under N_2 up to 600 °C. As seen, the thermal stability of the nonsulfonated graft copolymer was similar to that of PPO, with the decomposition starting just above 400 °C. The sulfonated copolymers were stable up to approximately 300 °C, at which point the sulfonate groups began to degrade, followed by the weight loss of the copolymer backbones above 400 °C. Figure 5b shows the thermal degradation of the copolymer membranes in the protonated form under N_2. The copolymers began to degrade at 220 °C, much lower than in the sodium salt form, with the degradation of the polymer chains remaining at approximately 400 °C. The membranes in the protonated form were also examined under air atmosphere and the $T_{d,5\%}$ values are shown in Table 2. As expected, the values were lower than those recorded under N_2, but followed the same trend. The degradation of the sulfonic acid groups began between 200 and 250 °C, and the polymer backbone degradation began at 300 °C.

Membrane Water Uptake and Proton Conductivity. The water uptake is an important parameter for the mechanical properties and proton conductivity of the membrane. Although the water is absorbed by the ionic phase, the level of water uptake is largely determined by the hydrophobic phase, and thus provides an insight into the continuity of the hydrophobic phase and its ability to counterbalance the osmotic pressure. Parameters that influence the water uptake include the IEC value, morphology, polymer chain flexibility (T_g) and molecular weight. In the present case, the water uptake was determined gravimetrically for the sulfonated PPO and PPOgPFS membranes according to eq 1, and was expressed as water content (wt %) and the molar ratio of water to sulfonic acid (λ), as seen in Table 2.

The copolymers s1PPOgPFS1 and s2PPOgPFS1 were both prepared from the same parent graft copolymer, but had different levels of sulfonation of the PPO backbone which produced membranes with IEC values of 1.2 and 1.4 mmol g^{-1}, respectively. As expected s2PPOgPFS1 showed a considerably higher water uptake (70 wt %) in relation to s1PPOgPFS1 (57 wt %), although at quite similar λ values. This may hint that the two membranes had a similar type of morphology. The difference in water uptake was also noted qualitatively, as the former membrane was much softer than the latter. Considering the membranes analyzed by TEM, sPPOgPFS3, sPPOgPFS2, and s1PPOgPFS1, there was an increase in the water uptake, from 32 to 57 wt %, as the PFS content decreased from 67 to 36 wt %. In addition, the λ value increased from 18 to 23 and 26, respectively. This reflects an increasing ability of the membranes to accommodate water as the morphology changed from cylindrical (sPPOgPFS3), via lamellar (sPPOgPFS2), to a lamellar arrangement with a more continuous ionic phase (s1PPOgPFS1). At an IEC value of 1.2 mmol g^{-1}, ungrafted sPPO was considerably less densely sulfonated than the PPO backbones of the graft copolymers at similar IEC values. Membrane sPPO thus did not contain any highly sulfonated phase and consequently had a comparatively low water uptake of 20 wt %, leading to $\lambda = 9$.

Figure 6 shows the proton conductivity of the membranes under immersed conditions between 20 and 120 °C. As seen, all the sulfonated graft copolymers had a significantly higher conductivity than sPPO at a similar IEC. The acid groups in sPPO are very much dispersed which leads to a quite low water uptake and an inability to form an efficient pathway for proton conduction. The proton conductivity of membrane sPPOgPFS3, containing 67 wt % PFS, was also fairly low. The membrane formed a morphology with the ionic phase organized as cylinders which lead to rather low water uptake. The conductivity of membranes with a cylindrical morphology can be expected to be high only if the cylinders are carefully oriented perpendicular to the membrane surface. At 56 wt % PFS, in membrane sPPOgPFS2, the morphology became lamellar which led to a significant increase in the water uptake and conductivity in relation to sPPOgPFS3. A further decrease in the PFS content to 36 wt %, in membrane s1PPOgPFS1, gave a morphology with a more continuous sulfonated phase which led to a further increase in the water uptake and proton conductivity. As mentioned above,

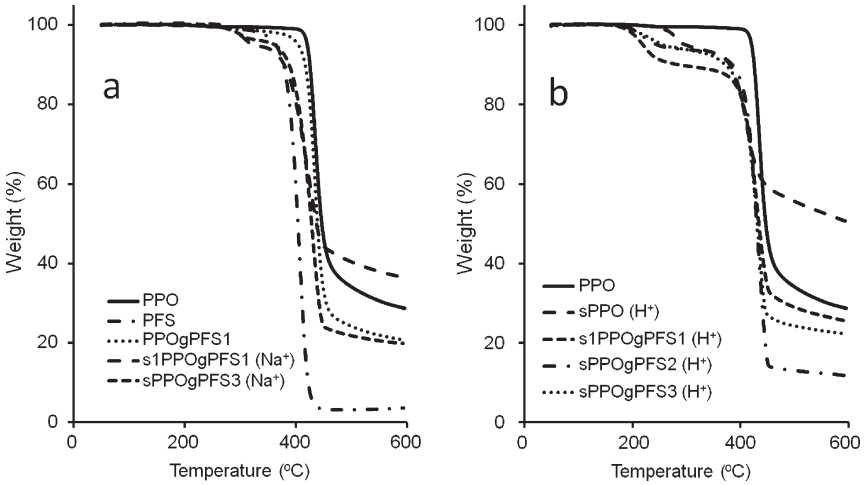

Figure 5. TGA traces of (a) PPO, PFS, and nonsulfonated and sulfonated PPOgPFS copolymers in the sodium form, and of (b) sulfonated PPO and PPOgPFS copolymers in the protonated form. The data was recorded at 10 °C min^{-1} under nitrogen.

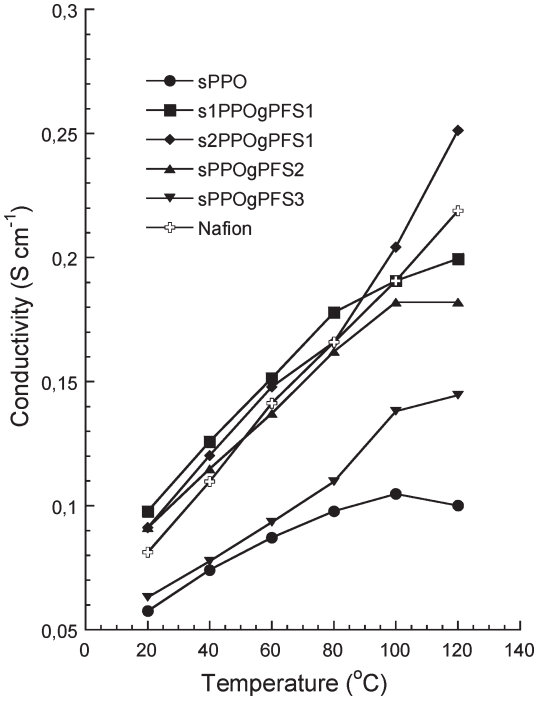

Figure 6. Conductivity data for the sulfonated PPO*g*PFS membranes measured by EIS under immersed conditions in a sealed cell from 20 to 120 °C. The corresponding data of sulfonated PPO and Nafion 117 was added for reference.

membrane s2PPOgPFS1 was based on the same parent graft copolymer as s1PPOgPFS1, but had a higher degree of sulfonation of the PPO backbone. The higher IEC gave a higher water uptake but a similar λ value as s1PPOgPFS1. The conductivity of membrane s2PPOgPFS1 was similar as s1PPOgPFS1 between 20 and 80 °C, but then increased to reach 0.25 S cm^{-1} at 120 °C. Possibly, the hydrophobic phase domain of membrane s2PPOgPFS1 was not able to counterbalance the forces of the osmotic pressure arising from the sulfonated PPO backbone. This morphological instability may have led to an excessive water uptake at high temperatures, resulting in increasing conductivity.

The phase separation and the higher concentration of sulfonic acid groups along the PPO backbone in the graft copolymers increased the connectivity of the ionic domains, in comparison with the sulfonated ungrafted PPO. Thus, the conductivity was enhanced without a drastic increase of the water uptake. Similar results were obtained by Holdcroft and co-workers after comparing the proton conductivity of linear sulfonated polystyrene with that of hydrophobic polystyrene carrying hydrophilic sulfonated polystyrene graft chains.[22] The present study show possibilities to prepare highly proton conducting membranes based on sulfonated polymers grafted with hydrophobic side chains—as opposed to hydrophobic polymers grafted with sulfonated side chains, which are more common.

CONCLUSIONS

Graft copolymers with highly sulfonated hydrophilic backbones and hydrophobic fluorinated side chains have been tailored and successfully prepared as proton conducting membrane materials. PFS side chains were grafted from an anionic PPO macroinitiator, followed by mild selective sulfonation of the PPO segments. The copolymers all had a similar density of PFS grafts along the PPO backbone, but the grafts had different chain lengths. Clear transparent and mechanically tough membranes were obtained by casting the copolymers from NMP solutions. The graft copolymers were shown to self-assemble into a variety of nanoscale morphologies, including lamellar and cylindrical arrangements, which depended on copolymer composition. In view of the solvent cast nature of the graft copolymer membranes, the nanophases had a regular size and were strikingly well-ordered with a seemingly high degree of long-range order. This may be a consequence of the presumably low polydispersity of the anionically polymerized PFS grafts. Thermal characterization by DSC confirmed the microphase separated nature of the membranes with a hydrophobic PFS phase and a highly sulfonated PPO phase, and TGA results showed that membranes in the protonated form started to degrade first at 220 °C under air atmosphere. As expected, the proton conductivity of the graft copolymer membranes depended on the IEC and the level of connectivity of the ionic phases resulting from the morphology. At a given IEC, the conductivity under fully humidified conditions of all the copolymer membranes exceeded that of an ungrafted sulfonated PPO membrane which demonstrated that

concentrating ionic groups to the backbone of a graft copolymer has a positive impact on the proton conductivity. Moreover, copolymers with a lamellar arrangement of the ionic phases produced conductivities similar to, or exceeding, that of Nafion. Thus, the work has shown that it is possible to prepare proton-exchange membranes with well-controlled morphology and high proton conductivity by employing graft copolymers with a sulfonated backbone bearing hydrophobic side chains.

■ ASSOCIATED CONTENT

Supporting Information. Figures showing SEC traces of unsulfonated and sulfonated PPO and graft copolymers in chloroform and DMF, respectively, and ^{1}H NMR and ^{19}F NMR spectra of PFS in $CDCl_3$. This material is available free of charge via the Internet at http://pubs.acs.org.

■ AUTHOR INFORMATION

Corresponding Author

*E-mail patric.jannasch@polymat.lth.se. Fax +46-46-222 4012.

■ ACKNOWLEDGMENT

We thank the Swedish Energy Agency and the Swedish Research Council for financial support. We are also grateful to Darryl Knight and Elizabeth Gillies of the University of Western Ontario, Canada, for the SEC analysis of the sulfonated copolymers.

■ REFERENCES

(1) de Bruijn, F. *Green Chem.* **2005**, *7*, 132–150.
(2) Zhang, J. L.; Xie, Z.; Zhang, J. J.; Tanga, Y. H.; Song, C. J.; Navessin, T.; Shi, Z. Q.; Song, D. T.; Wang, H. J.; Wilkinson, D. P.; Liu, Z. S.; Holdcroft, S. *J. Power Sources* **2006**, *160*, 872–891.
(3) Wieser, C. *Fuel Cells* **2004**, *4*, 245–250.
(4) Shao, Y. Y.; Yin, G. P.; Wang, Z. B.; Gao, Y. Z. *J. Power Sources* **2007**, *167*, 235–242.
(5) Maier, G.; Meier-Haack, J. *Adv. Polym. Sci.* **2008**, *216*, 1–62.
(6) Rozière, J.; Jones, D. J. *Annu. Rev. Mater. Res.* **2003**, *33*, 503–555.
(7) Li, Q. F.; He, R. H.; Jensen, J. O.; Bjerrum, N. J. *Chem. Mater.* **2003**, *15*, 4896–4915.
(8) Higashihara, T.; Matsumoto, K.; Ueda, M. *Polymer* **2009**, *50*, 5341–5357.
(9) Yang, Y. S.; Siu, A.; Peckham, T. J.; Holdcroft, S. *Adv. Polym. Sci.* **2008**, *215*, 55–126.
(10) Elabd, Y. A.; Hickner, M. A. *Macromolecules* **2011**, *44*, 1–11.
(11) Souzy, R.; Ameduri, B. *Prog. Polym. Sci.* **2005**, *30*, 644–687.
(12) Pang, J. H.; Zhang, H. B.; Li, X. F.; Wang, L. F.; Liu, B. J.; Jiang, Z. H. *J. Membr. Sci.* **2008**, *318*, 271–279.
(13) Karlsson, L. E.; Jannasch, P. *Electrochim. Acta* **2005**, *50*, 1939–1946.
(14) Lafitte, B.; Puchner, M.; Jannasch, P. *Macromol. Rapid Commun.* **2005**, *26*, 1464–1468.
(15) Lafitte, B.; Jannasch, P. *Adv. Funct. Mater.* **2007**, *17*, 2823–2834.
(16) Jutemar, E. P.; Jannasch, P. *J. Membr. Sci.* **2010**, *351*, 87–95.
(17) Einsla, M. L.; Kim, Y. S.; Hawley, M.; Lee, H. S.; McGrath, J. E.; Liu, B. J.; Guiver, M. D.; Pivovar, B. S. *Chem. Mater.* **2008**, *20*, 5636–5642.
(18) Tsang, E. M. W.; Zhang, Z.; Shi, Z.; Soboleva, T.; Holdcroft, S. *J. Am. Chem. Soc.* **2007**, *129*, 15106–15107.
(19) Tsang, E. M. W.; Zhang, Z. B.; Yang, A. C. C.; Shi, Z. Q.; Peckham, T. J.; Narimani, R.; Frisken, B. J.; Holdcroft, S. *Macromolecules* **2009**, *42*, 9467–9480.
(20) Norsten, T. B.; Guiver, M. D.; Murphy, J.; Astill, T.; Navessin, T.; Holdcroft, S.; Frankamp, B. L.; Rotello, V. M.; Ding, J. F. *Adv. Funct. Mater.* **2006**, *16*, 1814–1822.
(21) Ding, J. F.; Chuy, C.; Holdcroft, S. *Adv. Funct. Mater.* **2002**, *12*, 389–394.
(22) Ding, J. F.; Chuy, C.; Holdcroft, S. *Chem. Mater.* **2001**, *13*, 2231–2233.
(23) Cho, C. G.; Jang, H. Y.; You, Y. G.; Li, G. H.; An, S. G. *High Perform. Polym.* **2006**, *18*, 579–591.
(24) Burfield, D. R.; Gan, G. H.; Smithers, R. H. *J. Appl. Chem. Biotech.* **1978**, *28*, 23–30.
(25) Xu, T. W.; Wu, D.; Wu, L. *Prog. Polym. Sci.* **2008**, *33*, 894–915.
(26) Sugiyama, K.; Ishizone, T.; Hirao, A.; Nakahama, S. *Acta Polym.* **1995**, *46*, 424–431.
(27) Iojoiu, C.; Marechal, M.; Chabert, F.; Sanchez, J. Y. *Fuel Cells* **2005**, *5*, 344–354.
(28) Liang, M.; Jhuang, Y. J.; Zhang, C. F.; Tsai, W. J.; Feng, H. C. *Eur. Polym. J.* **2009**, *45*, 2348–2357.
(29) Cho, C. G.; Jang, H. Y.; You, Y. G.; Li, G. H.; An, S. G. *High Perform. Polym.* **2006**, *18*, 579–591.
(30) Chalk, A. J.; Hoogeboom, T. J. *J. Polym. Sci., Part A: Polym. Chem.* **1969**, *7*, 1359–1369.
(31) Chalk, A. J.; Hay, A. S. *J. Polym. Sci., Part A: Polym. Chem.* **1969**, *7*, 691–705.
(32) Ingratta, M.; Elomaa, M.; Jannasch, P. *Polym. Chem.* **2010**, *1*, 739–746.
(33) Marcelo, M.; Mendicuti, F.; Saiz, E.; Tarazona, M. P. *Macromolecules* **2007**, *40*, 1311–1320.
(34) Yang, S.; Gong, C.; Guan, R.; Zuo, H.; Dai, H. *Polym. Adv. Technol.* **2006**, *17*, 360–365.
(35) Fu, R.-Q.; Julius, D.; Hong, L.; Lee, J.-Y. *J. Membr. Sci.* **2008**, *322*, 331–338.
(36) Argun, A. A.; Ashcraft, J. N.; Hammond, P. T. *Polym. Prepr.* **2009**, *50*, 762–763.
(37) Canovas, M. J.; Sanz, S. J.; Ezquerra, T. A.; Linares, A. *Solid State Ionics* **2007**, *178*, 1049–1057.
(38) Peckham, T. J.; Holdcroft, S. *Adv. Mater.* **2010**, *22*, 4667–4690.
(39) Vukovic, R.; Karasz, F. E.; MacKnight, W. J. *Polymer* **1983**, *24*, 529–533.